

RESEARCH ARTICLE

Feasibility Study of NMR Based Serum Metabolomic Profiling to Animal Health Monitoring: A Case Study on Iron Storage Disease in Captive Sumatran Rhinoceros (*Dicerorhinus sumatrensis*)

Miki Watanabe^{1*}, Terri L. Roth⁴, Stuart J. Bauer¹, Adam Lane^{2,3}, Lindsey E. Romick-Rosendale¹

1 Division of Pathology, Cincinnati Children's Hospital Medical Center, Cincinnati, Ohio, United States of America, **2** Division of Experimental Hematology and Cancer Biology, Cancer and Blood Disease Institute, Cincinnati Children's Hospital Medical Center, Cincinnati, Ohio, United States of America, **3** Division of Biostatistics and Epidemiology, Cincinnati Children's Hospital Medical Center, Cincinnati, Ohio, United States of America, **4** Center for Conservation and Research of Endangered Wildlife, Cincinnati Zoo and Botanical Garden, Cincinnati, Ohio, United States of America

* Miki.Watanabe@cchmc.org



OPEN ACCESS

Citation: Watanabe M, Roth TL, Bauer SJ, Lane A, Romick-Rosendale LE (2016) Feasibility Study of NMR Based Serum Metabolomic Profiling to Animal Health Monitoring: A Case Study on Iron Storage Disease in Captive Sumatran Rhinoceros (*Dicerorhinus sumatrensis*). PLoS ONE 11(5): e0156318. doi:10.1371/journal.pone.0156318

Editor: James R. Connor, The Pennsylvania State University Hershey Medical Center, UNITED STATES

Received: February 25, 2016

Accepted: May 12, 2016

Published: May 27, 2016

Copyright: © 2016 Watanabe et al. This is an open access article distributed under the terms of the [Creative Commons Attribution License](https://creativecommons.org/licenses/by/4.0/), which permits unrestricted use, distribution, and reproduction in any medium, provided the original author and source are credited.

Data Availability Statement: All relevant data are within the paper and its Supporting Information files.

Funding: The authors have no support or funding to report.

Competing Interests: The authors have declared that no competing interests exist.

Abstract

A variety of wildlife species maintained in captivity are susceptible to iron storage disease (ISD), or hemochromatosis, a disease resulting from the deposition of excess iron into insoluble iron clusters in soft tissue. Sumatran rhinoceros (*Dicerorhinus sumatrensis*) is one of the rhinoceros species that has evolutionarily adapted to a low-iron diet and is susceptible to iron overload. Hemosiderosis is reported at necropsy in many African black and Sumatran rhinoceroses but only a small number of animals reportedly die from hemochromatosis. The underlying cause and reasons for differences in susceptibility to hemochromatosis within the taxon remains unclear. Although serum ferritin concentrations have been useful in monitoring the progression of ISD in many species, there is some question regarding their value in diagnosing hemochromatosis in the Sumatran rhino. To investigate the metabolic changes during the development of hemochromatosis and possibly increase our understanding of its progression and individual susceptibility differences, the serum metabolome from a Sumatran rhinoceros was investigated by nuclear magnetic resonance (NMR)-based metabolomics. The study involved samples from female rhinoceros at the Cincinnati Zoo (n = 3), including two animals that died from liver failure caused by ISD, and the Sungai Dusun Rhinoceros Conservation Centre in Peninsular Malaysia (n = 4). Principal component analysis was performed to visually and statistically compare the metabolic profiles of the healthy animals. The results indicated that significant differences were present between the animals at the zoo and the animals in the conservation center. A comparison of the 43 serum metabolomes of three zoo rhinoceros showed two distinct groupings, healthy (n = 30) and unhealthy (n = 13). A total of eighteen altered metabolites were identified in healthy versus unhealthy samples. Results strongly suggest that NMR-based

metabolomics is a valuable tool for animal health monitoring and may provide insight into the progression of this and other insidious diseases.

Introduction

Iron storage disease (ISD), the deposition of excess body iron into insoluble iron clusters in soft tissue, is a health concern in many species in captivity [1, 2]. The Sumatran rhinoceros (*Dicerorhinus sumatrensis*) is one of two browsing rhinoceros species that have evolutionarily adapted to a low-iron diet and is hence susceptible to iron overload [3]. It has been speculated that the lack of browse diversity and/or environmental conditions such as low exercise level and absence of hemoparasites are associated with the elevated metrics of iron loading in captive Sumatran rhinoceroses, however, the underlying cause of disease and the differences in individual susceptibility to ISD remain unclear [3, 4].

In humans, ISD or hemochromatosis is often associated with an autosomal recessive disorder caused by a mutation on the hemochromatosis (HFE) gene, which leads to increased iron absorption [5]. The HFE gene found in four rhinoceros species has been sequenced and mutations have been identified in two of the browser rhinoceros species [6]. However, a more recent study has challenged the relevance of this mutation as the underlying cause for ISD in captive rhinoceros species [7].

Most currently available diagnostic tests for animal disease rely on techniques such as a dipstick test, enzyme-linked immunoabsorbant assay (ELISA), or polymerase chain reaction (PCR). These methods all require the prior identification of target molecules, genes or proteins, and the development/validation of the detection method *e.g.* a specific antibody or primer for a species specific biomarker. Serum ferritin concentrations and transferrin saturation have been the two biomarkers most commonly employed to monitor iron loads in the rhinoceros [4]. Historically, these tests relied on an ELISA developed with antibodies to horse ferritin, but recently, an ELISA has been developed for Sumatran rhinos using monoclonal antibodies generated against Sumatran rhinoceros ferritin [8]. Regardless, serum ferritin concentrations may not be diagnostic of this disease because ferritin is an acute phase inflammatory protein and is not specific to ISD. Furthermore, the most accurate measurements require direct analysis of hepatic tissue [9] which is not feasible in a rhinoceros. Increases in serum transferrin saturation and ferritin levels have been shown to correlate with time in captivity in black rhinoceroses, however, the same has not been demonstrated for Sumatran rhinoceroses. Preliminary evidence suggests disparity in serum ferritin concentrations among Sumatran rhinoceroses in native and non-native habitats [4, 9]. In addition, the lack of knowledge regarding what normal (wild type) ferritin concentrations are and the maximum, healthy ferritin concentrations that a rhinoceros can tolerate creates another challenge in disease diagnosis. For these reasons, there is an urgent need to find other biomarkers specific to this disease that can be used for the development of diagnostic tests that are reliable, reproducible and applicable to any non-model animal species on a global basis.

Metabolomics monitors the alterations in metabolite concentrations caused by stimuli in given biological samples and has been demonstrated as a useful tool in many areas such as medical, environmental, and basic biological research [10–14]. This approach provides untargeted and comprehensive profiles of small molecules in body fluids and/or tissue extracts. The comparison of metabolic signatures can be used to identify differences due to age, gender, disease development, drug treatments, diets and living environments. One of the advantages of using this approach is that neither a specific marker for each condition nor species specific databases are required. Metabolomics has the potential to be more suitable over currently

available tools for health monitoring of non-model species such as protected or endangered animals. This potential has been demonstrated in several species such as fish [15, 16], crustaceans [17, 18], mussels [19–21], whale sharks [22], and black bears [23]. In addition, metabolomics analyses provide a large amount of information from samples that can be obtained by non-lethal and minimally invasive methods e.g. urine, feces, and blood.

The objectives of this study are to demonstrate the ability of NMR-based metabolomics to differentiate the health status of individual Sumatran rhinoceroses and to identify metabolites that are altered during disease onset and/or progression. In addition, the effect of the living environment on the serum metabolome is assessed in this study using samples collected from seven individual Sumatran rhinoceros from two locations, the Cincinnati Zoo and Botanical Garden in Cincinnati, Ohio and the Sumatran Rhinoceros Conservation Centre in Peninsular Malaysia.

Materials and Methods

Serum samples

The serum samples analyzed in this study were obtained opportunistically from a bank of samples previously collected from seven female Sumatran rhinoceros between years 1997 to 2014 (Table 1) as part of their regular health monitoring program. Because so few Sumatran rhinoceros currently exist, serial samples collected over time from the same individuals were used to observe the alteration in the serum metabolome during disease development. To avoid the potential influences that gender may have on the serum metabolome, only female rhinoceros were profiled for this study. One sample from each of four female Sumatran rhinoceroses (Rhino-4, Rhino-5, Rhino-6 and Rhino-7) maintained in captivity at the Sungai Dusun Sumatran Rhinoceros Conservation Centre (SRCC) in Peninsular Malaysia were analyzed in this study to determine if serum metabolomes of this species are affected by environmental differences such as habitats/diets. Multiple samples collected over several years from three rhinoceroses maintained at the Cincinnati Zoo, (Rhino-1, Rhino-2 and Rhino-3) were analyzed for differences between healthy and unhealthy states. Two of the animals, Rhino-1 and -2 died from hemochromatosis. The healthy sample group in this study included samples from Rhino-3, a healthy control animal (n = 5), as well as the samples from Rhino-1 (n = 14) and Rhino-2 (n = 11) collected 11 months and 2 years prior to any clinical signs of hemochromatosis, respectively. Rhino-1 (n = 10), and Rhino-2 (n = 3) samples collected after diagnosis were categorized as unhealthy.

Sample Collection

Female Sumatran rhinoceroses at the Cincinnati Zoo were trained through operant conditioning to allow blood collection from the veins that run along the back of the ears. Rhinoceroses at

Table 1. List of samples from Sumatran rhinoceroses used in this study.

Sample	Gender	Living environment	Sample collection year			
			Healthy	n	Sick	n
Rhino_1	F	Cincinnati zoo, OH	2000–2012	14	2013–2014	10
Rhino_2	F	Cincinnati zoo, OH	1997–2008	11	2009	3
Rhino_3	F	Cincinnati zoo, OH	1997–2000	5		
Rhino_4	F	The Sumatran Rhinoceros Conservation Centre, Malaysia	2003	1		
Rhino_5	F	The Sumatran Rhinoceros Conservation Centre, Malaysia	2003	1		
Rhino_6	F	The Sumatran Rhinoceros Conservation Centre, Malaysia	2003	1		
Rhino_7	F	The Sumatran Rhinoceros Conservation Centre, Malaysia	2003	1		

doi:10.1371/journal.pone.0156318.t001

the SRCC in Malaysia were conditioned for blood collection from a lateral vein in the tail. No sedation or anesthesia was necessary, and animals were not fasted prior to blood collection. A tourniquet was placed at the base of the ear or base of tail, and a 23-gauge butterfly catheter was inserted into the vein. Blood from the ear vein was collected into a 6 mL syringe and emptied into a red top serum separator collection tube. Blood from the tail was collected directly in the vacutainer red top serum separator tube. After approximately 30–60 minutes, samples were centrifuged (1300 xg) and the recovered serum stored in ~1.0 mL aliquots at -80°C until they were thawed for analysis.

Sample preparation

To obtain both polar and non-polar fractions of the serum for future analysis, all samples were extracted using a modified Bligh and Dyer extraction method. Methanol-chloroform-water extraction of the serum samples was performed as previously described [24]. Briefly, the appropriate volumes of solvents (final constant ratio of 2:2:1.8 of chloroform: methanol: water) were added to serum samples [25, 26]. The top layer, i.e. the hydrophilic extract, was dried in a vacuum centrifuge for approximately 2 hrs at room temperature and stored at -80°C until further preparation for NMR data collection. On the day of the data collection, dried polar extracts were re-hydrated with 600 μL of NMR buffer containing 100 mM phosphate buffer, pH 7.3, 1 mM TMSP (3-Trimethylsilyl 2,2,3,3- d_4 propionate, CAS 24493-21-8), and 1 mg/mL NaN_3 (sodium azide CAS 26627-22-8) prepared in D_2O . A 550 μL aliquot of each sample was then transferred into 5 mm NMR tubes (Norell).

Quality control

To assess the reproducibility of the sample extraction, sample stability and analytical methods, quality control samples were prepared and analyzed along with the test samples. In-house prepared pooled human plasma control material (PCM) samples and a solvent blank sample were extracted with test samples in each batch. In total, five PCM samples and blank samples were extracted in this study.

Data collection

One-dimensional ^1H NMR spectra were recorded on all samples using the Carr-Purcell-Meiboom-Gill (CPMG) pulse sequence with presaturation of the water peak on a 600 MHz INOVA spectrometer. Experiments were run with 4 dummy scans (DS) and 256 acquisition scans (NS) with an acquisition time (AQ) of 2.09s, a relaxation delay (D1) of 4.0s and a mixing time was 60ms. The spectral width was 26 ppm, and 64K real data points were collected. Two-dimensional ^{13}C edited heteronuclear single quantum correlation (HSQC) spectra for representative samples were acquired. For HSQC data, a relaxation delay equal to 1.5s was used between acquisitions and a refocusing delay of 3.45ms was implemented. In general, 3584 data points in the direct dimension and 360 data points in the indirect dimension with 144 scans per increment were acquired with spectral widths of 26 ppm in F2 and 83 ppm in F1 (^{13}C). All NMR data were processed using Topspin 3.1 software (Bruker Analytik, Rheinstetten, Germany). All FIDs were subjected to an exponential line-broadening of 0.3 Hz. Upon Fourier transformation, each spectrum was manually phased, baseline corrected, and referenced to the internal standard TMSP at 0.0 ppm.

Statistical analysis

Principal components analysis (PCA) was performed to determine the reproducibility of the extraction and sample stability and to look for metabolic differences in the Sumatran rhinoceros

population pre- and post-disease onset. From ^1H NMR spectra, spectral bin intensities tables were generated using AMIX (version 3.9.11; Bruker Biospin Inc., Billerica, MA). The spectra from 0.5 to 10.0 ppm, excluding the region of the residual water resonance (4.7–4.9 ppm) and contaminants identified in the blanks, methanol (3.35–3.36 ppm) and chloroform (7.67–7.69 ppm), were reduced into 980 uniform bins in 0.01 ppm wide. Signal intensities were summed for integration, and the spectra were normalized to constant total intensity of the spectral area. PCA analyses were performed using the spectral bin intensities tables (S1 File). The scores from each PCA analysis were exported to Microsoft Excel and differences between groups were based on PC1 and PC2 scores were assessed using Student t-tests. Though data is not presented, the autocorrelation and partial autocorrelation function plots were performed on PC1 and PC2 scores using JMP12 software (SAS Institute Inc., Cary, NC).

The spectral bin intensities tables were further analyzed using a univariate approach, based on bin-by-bin differences between healthy and unhealthy animals' spectra. In order to identify the NMR peaks that are significantly different between healthy and unhealthy samples, ^1H significant difference spectra (SDS) were generated [16, 17]. Pairwise differences within each bin were compared using Student's t-test. The false discovery rate (FDR) was controlled at 0.05 level using the Benjamini Hochberg method [27]. The SDS plot was generated by taking the mean difference between the two groups, healthy vs. unhealthy. Metabolites were assigned to those significant bins based on the chemical shifts as described below.

Metabolite assignments

Metabolites found in serum polar extracts were assigned based on one-dimensional (1D) ^1H and two-dimensional (2D) ^1H - ^{13}C NMR experiments. Peaks were assigned by comparing the chemical shifts and spin-spin couplings with reference spectra found in databases, such as the Human Metabolome Database (HMDB)[28], the Madison metabolomics consortium database (MMCD)[29], the biological magnetic resonance data bank (BMRB)[30], and Chemomx® NMR Suite profiling software (Chemomx Inc. version 8.1).

Serum ferritin assay

Serum samples from Rhino-1 (n = 28) and Rhino-2 (n = 16) collected over a period of 8 and 7 years, respectively, were analyzed for ferritin concentrations by Kansas State University. The enzyme immunoassay employs an equine anti-ferritin antibody (S-6146, Sigma Aldrich) and black rhino ferritin as a standard and was previously validated for measuring circulating concentrations of ferritin in black rhinos [31].

Results and Discussion

Metabolic differences between healthy and unhealthy Sumatran rhinoceroses

To our knowledge this study is the first attempt to characterize metabolomic changes associated with hemochromatosis in any wildlife species. Comparisons of metabolic profiles among three zoo animals were assessed in PCA scores plot (Fig 1A and 1B). The first component (PC1) in PCA scores plot separated the healthy samples from unhealthy samples from Rhino-1 (PC1: $p = 8.73 \times 10^{-7}$) and Rhino-2 (PC1: $p = 3.59 \times 10^{-2}$) (Fig 1B). The separation in PC2 direction between the unhealthy animals is most likely caused by individual differences with regard to factors like the progression of disease, age, and development of secondary problems associated with hemochromatosis progression (e.g. compromised liver and/or renal function and overall body wasting).

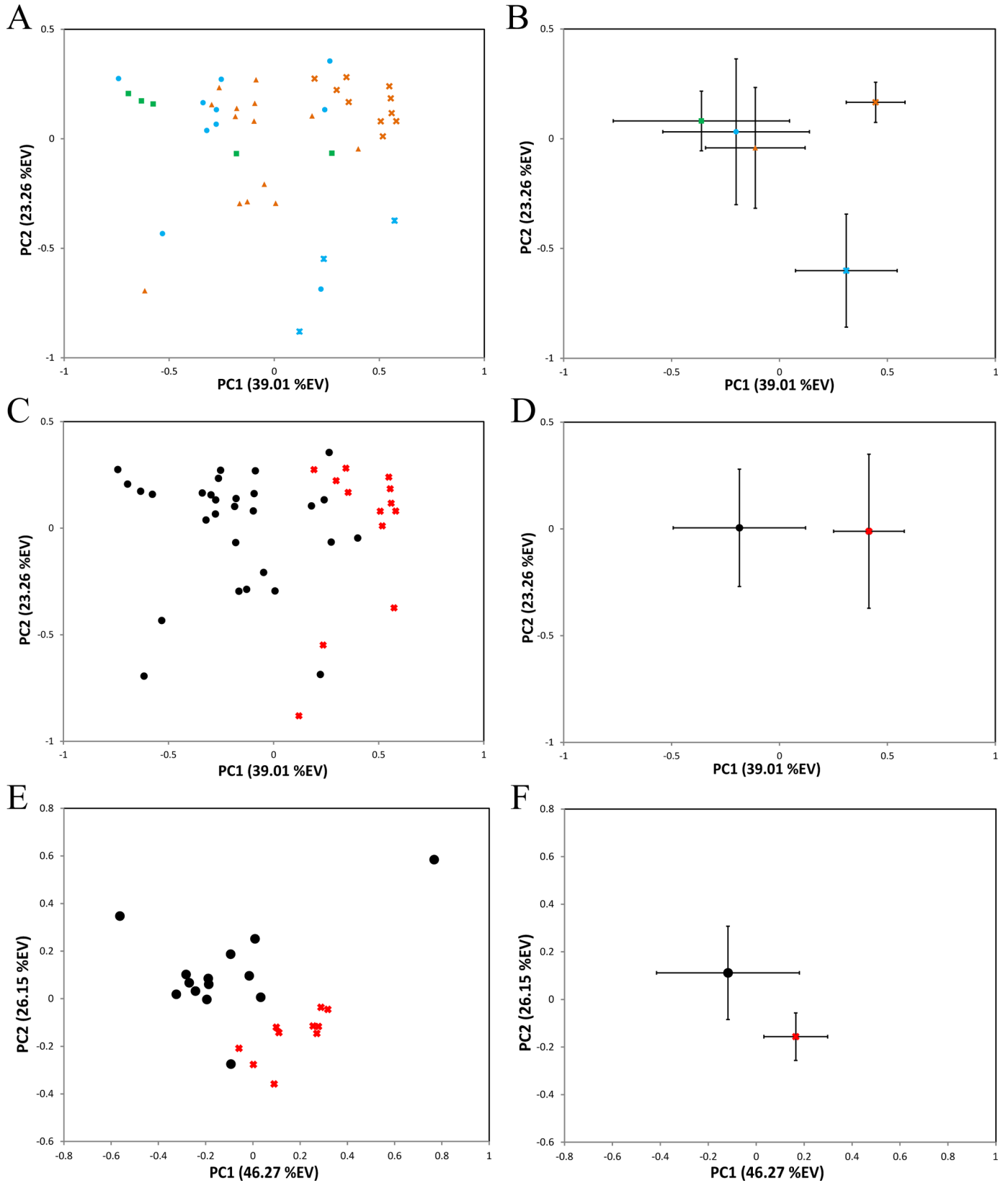


Fig 1. Multivariate PCA analysis of serum metabolome from Sumatran rhinoceroses. (A) PCA scores plots indicating the relationship between three rhinoceroses: Rhino-1 (red), Rhino-2 (blue), Rhino-3 (green), and their health status (x-healthy, ●-unhealthy). (B) The average PC scores of each animal corresponding to the plot (A). The error bars are indicating the standard deviations. (C) PCA scores plot (A) based on the health status of animals (x-Healthy-black, ●-Unhealthy). (D) The average scores of each animal corresponding to the plot (C). (E) PCA scores plots indicating the Rhino-1 health status (x-healthy, ●-unhealthy), and the average PC scores (F).

doi:10.1371/journal.pone.0156318.g001

The clustering of the two study groups, healthy and unhealthy, became more apparent upon the removal of the identity of the animals (Fig 1C and 1D). The separation in PC1 direction seems to indicate the presence of metabolic differences between all the healthy and unhealthy samples, however, other potential factors including individual animal's differences unbalanced number of samples in each group, *etc.* may influence this result. For this reason, further analysis was performed on samples only from Rhino-1, which had the largest number of samples from one animal. In the PCA analysis of Rhino-1 samples, a clear grouping was observed based on the health status (Fig 1E and 1F), no time correlation based on the progression of the disease was observed in these samples (data not shown). The separation between the healthy and unhealthy samples were significant based on the Student's t-test in both PC1 ($p = 5.40 \times 10^{-3}$) and PC2 ($p = 2.77 \times 10^{-4}$).

Metabolic changes during the disease development and progression

The univariate analysis of significant difference spectra (SDS) revealed 178 bins out of 980 bins with statistically significant differences between healthy and unhealthy groups (Fig 2). Significant metabolites were assigned based on these SDS bins and 1D and 2D NMR spectral annotations. A total of 18 metabolites differed in relative intensities between healthy and unhealthy animal samples (Table 2).

Significant decreases in branched-chain amino acids ((BCAAs) leucine, isoleucine, and valine) were observed in unhealthy samples from Rhino-1 and -2 compared to healthy samples (Fig 3A–3C). The high clearance rate of plasma BCAAs in humans with liver cirrhosis has been identified previously [32]. A number of studies have demonstrated the benefits of BCAA supplementations in albumin synthesis [33], nutritional status [34], glucose metabolism [35, 36], and decreasing the frequency of hepatocellular carcinoma [37]. More recently, the oral supplementation of BCAA has been shown to reduce hepatic iron accumulation and oxidative stress in mice [38].

In addition to the decrease in BCAA, the increase in circulating aromatic amino acids (AAA) has been reported in several cases of hepatic failure [39–42]. The decrease in Fischer-ratio (BCAA/AAA ratio) is suggested to be due to the induction of muscle catabolism and reduction in AAA breakdown in the dysfunctional liver [43]. The observation of increased phenylalanine levels (Fig 3D) along with the rapid clearance of BCAA in both the Rhino-1 and -2 unhealthy samples strongly correlate with these previous observations in liver failure associated with hepatic encephalopathy.

Significant decreases in creatine, creatinine (Fig 3E), and phosphocreatine (Fig 3F) were identified in unhealthy samples (Table 1). Though there are limitations in the use of serum creatinine concentrations as a tool for monitoring liver disease [44], it has been incorporated into the panel of tests employed to monitor the decline of hepatic function in humans [45–47]. Based on these results that indicate reduced creatine, phosphocreatine and creatinine concentrations along with altered BCAA and AAA in serum collected from rhinoceroses in liver failure, it may be prudent to include tests for these metabolites when monitoring rhinoceroses with suspected liver problems.

Reproducibility across multiple aspects of the study is a key to both the overall success of the study and also to the ability to interpret the results obtained. To assess the reproducibility

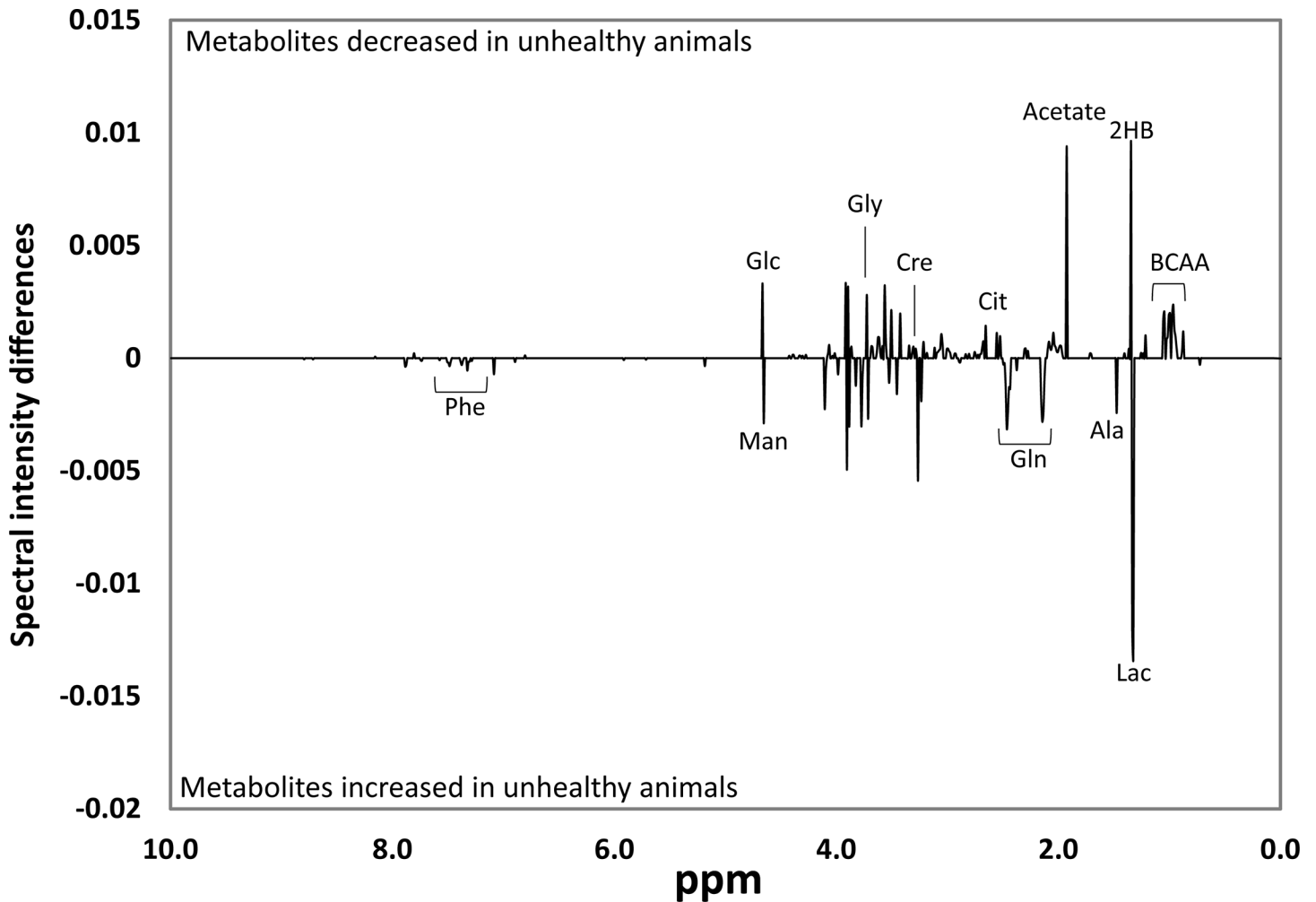


Fig 2. Univariate significant difference spectra (SDS) analysis. SDS spectra obtained by subtracting the mean buckets ($n = 980$) of the unhealthy from healthy samples. Only the buckets ($n = 178$) with significant alterations based on t-test with FDR correction are plotted. BCAA: branched chain amino acids, 2HB: 2-hydroxyisobutyrate, Lac: lactate, Ala: alanine, Gln: glutamine, Cit: citrate, Cre: creatine, Gly: glycine, Glc: glucose, Man: mannose, Phe: phenylalanine.

doi:10.1371/journal.pone.0156318.g002

of the sample extraction, sample stability and analytical methods, quality control samples were prepared and analyzed along with the test samples. The PCA analysis of all the samples in this study indicated the high repeatability of the sample processing and analytical methods (S1 Fig). The spectral median relative standard deviation [48] of PCM was determined to be 13.02%.

As the metabolic signature of the Sumatran Rhino had not previously been studied, we not only investigated the metabolic differences between the healthy and unhealthy samples, but also attempted to gain insight into the most abundant metabolites present in rhinoceros serum. A total of 34 metabolites were assigned based on the 1D and 2D HSQC NMR experiments (S2 Fig) and the representative spectra demonstrates the complexity that arises from the untargeted approach at investigating the polar serum metabolites.

In addition to understanding the metabolic differences associated with the diseased state, we were also interested in investigating the degree of separation that might occur between the metabolomes of rhinoceroses in different environments with different diets knowing that such variables can be significant confounding factors in metabolomics studies. Assessments of

Table 2. List of metabolites that were altered significantly in unhealthy compared to healthy rhino serum samples after FDR correction.

Metabolites ^a	Bin ^b (ppm)	P value ^c (FDR Corr)	Changes ^d	Function
Ile	1.015	1.02E-11	↓	Essential amino acid, BCAA, protein catabolism
Val	1.055	8.10E-10	↓	Essential amino acid, BCAA, protein catabolism
Gly	3.565	2.59E-03	↓	Amino acid metabolism
Leu	0.955	1.04E-05	↓	Essential amino acid, BCAA, protein catabolism
Gln	2.145	3.46E-05	↑	Amino acid metabolism
Asn	2.885	1.74E-03	↓	Amino acid metabolism
Ala	1.475	9.02E-05	↑	Amino acid metabolism
Phe	7.325	9.61E-06	↑	Essential amino acid, AAA,
Mannose	5.185	9.57E-07	↑	Carbohydrate sugar, Glycoprotein
Glucose	5.235	1.55E-03	↓	Carbohydrate sugar
Creatine	3.045	5.21E-03	↓	Creatinine synthesis in liver
Phosphocreatine	3.055	1.00E-07	↓	Creatinine synthesis in liver
Creatinine	4.065	1.81E-06	↓	Creatinine synthesis in liver
Pyruvate	2.375	2.20E-05	↑	Krebs cycle
Citrate	2.525	2.41E-08	↓	Krebs cycle, Fatty acid synthesis
Lactate	4.105	5.25E-07	↑	Krebs cycle
2-Hydroxyisobutyrate	1.365	8.61E-08	↓	
Acetate	1.925	1.71E-06	↓	

^a Ile: isoleucine, Val: valine, Gly: glycine, Leu: leucine, Gln: glutamine, Asn: asparagine, Ala: alanine, Phe: phenylalanine.

^b The chemical shift of the bin used for the p value calculation.

^c The FDR corrected alpha values.

^d Increased (↑) and decreased (↓) in unhealthy samples compared to healthy samples.

doi:10.1371/journal.pone.0156318.t002

metabolic differences due to the living environment were performed by comparing healthy samples from the Sumatran rhinoceroses at the Cincinnati Zoo and those from the rhinoceroses at the SRCC (S3 Fig). The grouping of three zoo animals (Rhino-1 through -3) suggested that the effects from difference in ages of animal, time of collections (season/ year), or in diet within the zoo on serum metabolome are minimal. The largest separation was found in PC1 ($p = 7.67 \times 10^{-5}$) between the animals in the SRCC (Rhino-4 through -7) and the zoo (Rhino-1 through -3), indicating the different countries had the most profound impact on metabolomic differences, most likely due to very different browse diets being fed.

Finally, the sensitivity of the NMR-based metabolomics assay was compared to the currently available assays. The serum ferritin concentrations of Rhino-1 and Rhino-2 were evaluated over time (S4 Fig). Though the overall trends show increased levels of ferritin in both animals following disease diagnosis, significant fluctuations were also observed during period that the animals were healthy. These observations emphasize the difficulty in diagnosing ISD in the rhinoceros species by the traditional methods, and highlight the need for additional diagnostic assays that can be used both in combination with serum ferritin monitoring or as stand-alone surveillance techniques

Conclusion

The measurement of serum ferritin concentrations via ELISA currently is the primary method employed for monitoring total body iron load and the progression of ISD in the rhinoceros. Although serum ferritin does increase in Sumatran rhinoceroses suffering from

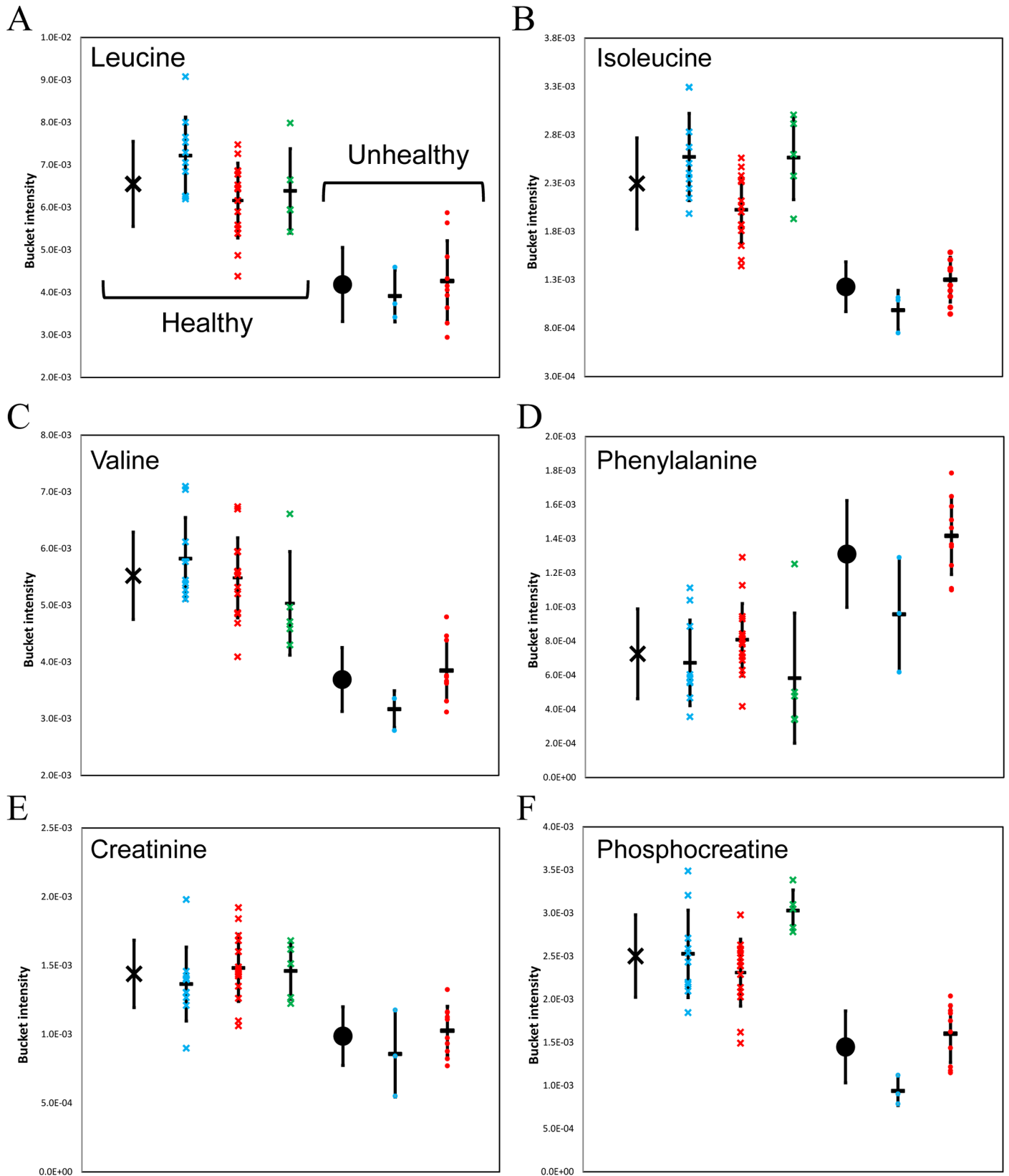


Fig 3. Metabolite changes in relation to health status of rhinoceroses. Bucket intensities of each altered metabolite from three rhinoceroses: Rhino-1 (red), Rhino-2 (blue), Rhino-3 (green), and their health status (x-healthy, •-unhealthy). The averages of all healthy or unhealthy samples are shown in black. (A) leucine, (B) isoleucine, (C) valine, (D) phenylalanine, (E) creatinine, (F) phosphocreatine.

doi:10.1371/journal.pone.0156318.g003

hemochromatosis, its value as a diagnostic biomarker of this disease in this species has recently been questioned [8]. Therefore, the identification of other biomarkers that could provide a more definitive diagnosis would be of great value for the rhinoceros and other wildlife species susceptible to this disease. Data generated in this study are encouraging and suggest that metabolomics can play an important role in helping to identify potential biomarkers of disease progression and/or organ dysfunction in wildlife. Ferritin is one of the main intercellular iron storage proteins and the increased level of ferritin has been observed during the ISD development in multiple species including rhinoceros. Ferritin level is regulated through porphyrin metabolism pathway which includes heme protein synthesis. As both glycine and BCAA are involved in this pathway, the significant decrease in this combination of amino acids may also be due to the alteration in ferritin production. The induction of ferritin production due to the high level of free-iron, could be utilizing all the free glycine and BCAA in the pool. The primary cause of these alterations in the serum metabolome of unhealthy rhinoceroses remains unknown.

In order to pinpoint the cause of ISD, additional studies that include both larger sample sizes and a more diverse sampling from multiple animals is needed. In spite of the noted limitations, this study has successfully demonstrated the capability of NMR-based metabolomics to detect changes in the health of a non-model species, the Sumatran rhinoceros. Alterations of 18 serum metabolites, many of which have previously been linked to liver dysfunction in other species, were observed in the unhealthy animals. The specificity of the observed metabolic changes to the development of ISD will be investigated with a study consisting of a larger population size. Although the declining rhinoceros species population makes increasing the sample size challenging, it also highlights the importance of this type of study in helping to ultimately reduce the number of rhinoceros deaths. Nonetheless, the results here indicate that the serial monitoring of the blood metabolome over an extended period of time would allow each animal to serve as its own control to evaluate health status. This time-series analysis approach for monitoring metabolic changes during disease progression may lead to the development of new diagnostic methods in non-model species.

Supporting Information

S1 Fig. Quality control assessment. PCA score plot of test samples and quality control (QC) samples used in this study. Identical pooled plasma samples (PCM) were extracted along with the study samples in each batch. Total of 5 PCM (+) and 47 test samples: Rhino-1(x, red), Rhino-2(•, blue), Rhino-3(Δ, green), Rhino-4~7(◆, yellow), were extracted in this study. The PCA scores plot and the calculated relative standard deviation (RSD) of the PCM (13.02%) indicated a high degree of reproducibility between the extraction batches (PDF)

S2 Fig. Serum metabolome of Sumatran rhinoceros (*Dicerorhinus sumatrensis*). A representative ¹H NMR spectrum of serum polar extract from Sumatran rhinoceros and metabolite assignments that have been confirmed with 2D HSQC NMR experiments in two sections A) 0.5–4.6ppm, and B) 5.0–8.6ppm. Assignments: 1) 2-hydroxyvalerate, isoleucine, leucine, valine, 2) isobutyrate, 3) propylene glycol, 4) 3-hydroxybutyrate, 5) 3-hydroxyisovalerate, 6) lactate, 7) 2-hydroxyisobutyrate, 8) alanine, 9) suberate, 10) lysine, 11) acetate, 12) glutamate, 13) succinate, pyruvate, 14) glutamine, 15) citrate, 16) asparagine, 17) creatine,

phosphocreatine, 18) histidine, 19) betaine, 20) glycine, 21) threonine, 22) mannose, 23) glucose, 24) tyrosine, 25) phenylalanine, 26) hippurate, 27) tryptophan, 28) benzoate, 29) formate. (PDF)

S3 Fig. Environmental effect in Sumatran rhinoceros serum metabolome. PCA scores plot (A) and the PCA score average (B) of serum samples from the animals maintained at the Cincinnati Zoo, USA, Rhino-1(x), Rhino-2(●), Rhino-3(Δ-green), and the Sumatran Rhino Conservation Center, Malaysia, Rhino-4~7(◆-yellow) indicating the metabolic differences associated with the different living environment. (PDF)

S4 Fig. The serum ferritin concentrations from captive rhinoceroses. The changes in serum ferritin concentrations from Rhino-1 (◆) and Rhino-2 (●) are plotted over time. The disease diagnostic time point is indicated by the (*) for both animals and the health status is indicated in black (healthy) and red (sick). Though the sampling time period overlaps with that for samples analyzed in this study, the samples were not all identical matches due to the limited amount of samples available from any given date. (PDF)

S1 File. The spectral bin table of all the Sumatran rhinoceroses serum samples used in this study. (ZIP)

Acknowledgments

The authors would like to thank Tracey B. Schock for her valuable guidance. The authors also would like to acknowledge the Department of Wildlife and National Parks, Peninsular, Malaysia for permitting the use of the samples and Dr. Aidi Mohamad of the Malaysian Rhino Foundation for collecting the blood samples. In addition, the authors thank the Cincinnati Zoo & Botanical Garden veterinary and keeper staff who collected and banked the serum samples on all of the Sumatran rhinos maintained at the zoo. Finally, the authors would like to acknowledge the Shared Facilities at Cincinnati Children's Hospital Medical Center and Research Foundation for their instrumentation supports.

Author Contributions

Conceived and designed the experiments: MW TLR. Performed the experiments: MW SJB TLR. Analyzed the data: MW AL TLR. Contributed reagents/materials/analysis tools: MW LER. Wrote the paper: MW SJB AL LER TLR.

References

1. Dierenfeld ES, Atkinson S, Craig AM, Walker KC, Streich WJ, Clauss M. Mineral concentrations in serum/plasma and liver tissue of captive and free-ranging Rhinoceros species. *Zoo Biology*. 2005; 24(1):51–72. doi: [10.1002/zoo.20043](https://doi.org/10.1002/zoo.20043)
2. Clauss M, Paglia DE. Iron storage disorders in captive wild mammals: the comparative evidence. *Journal of zoo and wildlife medicine: official publication of the American Association of Zoo Veterinarians*. 2012; 43(3 Suppl):S6–18. Epub 2012/11/20. doi: [10.1638/2011-0152.1](https://doi.org/10.1638/2011-0152.1) PMID: [23156701](https://pubmed.ncbi.nlm.nih.gov/23156701/).
3. Dierenfeld ES, Kilbourn A, Karesh W, Bosi E, Andau M, Alsisto S. Intake, utilization, and composition of browses consumed by the Sumatran rhinoceros (*Dicerorhinus sumatrensis harissoni*) in captivity in Sabah, Malaysia. *Zoo Biology*. 2006; 25(5):417–31. doi: [10.1002/zoo.20107](https://doi.org/10.1002/zoo.20107)
4. Candra D, Radcliffe RW, Khan M, Tsu IH, Paglia DE. Browse Diversity And Iron Loading In Captive Sumatran Rhinoceroses (*Dicerorhinus Sumatrensis*): A Comparison Of Sanctuary And Zoological Populations. *Journal of Zoo and Wildlife Medicine*. 2012; 43(3s):S66–S73. doi: [10.1638/2011-0127.1](https://doi.org/10.1638/2011-0127.1)

5. Feder JN, Gnirke A, Thomas W, Tsuchihashi Z, Ruddy DA, Basava A, et al. A novel MHC class I-like gene is mutated in patients with hereditary haemochromatosis. *Nature genetics*. 1996; 13(4):399–408. Epub 1996/08/01. doi: [10.1038/ng0896-399](https://doi.org/10.1038/ng0896-399) PMID: [8696333](https://pubmed.ncbi.nlm.nih.gov/8696333/).
6. Beutler E, West C, Speir JA, Wilson IA, Worley M. The HFE Gene of Browsing and Grazing Rhinoceroses: A Possible Site of Adaptation to a Low-Iron Diet. *Blood Cells, Molecules, and Diseases*. 2001; 27(1):342–50. <http://dx.doi.org/10.1006/bcmd.2001.0386>. PMID: [11358396](https://pubmed.ncbi.nlm.nih.gov/11358396/)
7. Olias P, Mundhenk L, Bothe M, Ochs A, Gruber AD, Klopffleisch R. Iron overload syndrome in the black rhinoceros (*Diceros bicornis*): microscopical lesions and comparison with other rhinoceros species. *Journal of comparative pathology*. 2012; 147(4):542–9. Epub 2012/09/01. doi: [10.1016/j.jcpa.2012.07.005](https://doi.org/10.1016/j.jcpa.2012.07.005) PMID: [22935088](https://pubmed.ncbi.nlm.nih.gov/22935088/).
8. Roth TL. Development of a rhino ferritin specific assay for monitoring the progression of iron overload disorder in Sumatran rhinos (*Dicerorhinus sumatrensis*). *Proceedings Workshop on Iron Overload Disorder in Browsing Rhinoceros*, Progress Report, Pp14–15, Orlando, FL: 2016.
9. Paglia DE, Tsu IH. Review of laboratory and necropsy evidence for iron storage disease acquired by browser rhinoceroses. *Journal of zoo and wildlife medicine: official publication of the American Association of Zoo Veterinarians*. 2012; 43(3 Suppl):S92–104. Epub 2012/11/20. doi: [10.1638/2011-0177.1](https://doi.org/10.1638/2011-0177.1) PMID: [23156711](https://pubmed.ncbi.nlm.nih.gov/23156711/).
10. Bundy J, Davey M, Viant M. Environmental metabolomics: a critical review and future perspectives. *Metabolomics*. 2009; 5(1):3–21. doi: [10.1007/s11306-008-0152-0](https://doi.org/10.1007/s11306-008-0152-0)
11. Nicholson JK, Connelly J, Lindon JC, Holmes E. Metabonomics: a platform for studying drug toxicity and gene function. *Nature reviews Drug discovery*. 2002; 1:153–61.
12. Nicholson JK, Wilson ID, Lindon JC. Pharmacometabonomics as an effector for personalized medicine. *Pharmacogenomics*. 2011; 12(1):103–11. Epub 2010/12/23. doi: [10.2217/pgs.10.157](https://doi.org/10.2217/pgs.10.157) PMID: [21174625](https://pubmed.ncbi.nlm.nih.gov/21174625/).
13. Spratlin JL, Serkova NJ, Eckhardt SG. Clinical applications of metabolomics in oncology: a review. *Clinical cancer research: an official journal of the American Association for Cancer Research*. 2009; 15:431–40.
14. Kaddurah-Daouk R, Kristal BS, Weinshilboum RM. Metabolomics: a global biochemical approach to drug response and disease. *Annual review of pharmacology and toxicology*. 2008; 48:653–83. Epub 01/11. doi: [10.1146/annurev.pharmtox.48.113006.094715](https://doi.org/10.1146/annurev.pharmtox.48.113006.094715) PMID: [18184107](https://pubmed.ncbi.nlm.nih.gov/18184107/).
15. Southam AD, Easton JM, Stentiford GD, Ludwig C, Arvanitis TN, Viant MR. Metabolic changes in flatfish hepatic tumours revealed by NMR-based metabolomics and metabolic correlation networks. *Journal of proteome research*. 2008; 7:5277–85. doi: [10.1021/pr800353t](https://doi.org/10.1021/pr800353t) PMID: [19367724](https://pubmed.ncbi.nlm.nih.gov/19367724/).
16. Schock TB, Newton S, Brenkert K, Leffler J, Bearden DW. An NMR-based metabolomic assessment of cultured cobia health in response to dietary manipulation. *Food Chem*. 2012; 133(1):90–101. PMID: [WOS:000301826400013](https://pubmed.ncbi.nlm.nih.gov/WOS:000301826400013/).
17. Schock TB, Duke J, Goodson A, Weldon D, Brunson J, Leffler JW, et al. Evaluation of Pacific White Shrimp (*Litopenaeus vannamei*) Health during a Superintensive Aquaculture Growout Using NMR-Based Metabolomics. *PLoS One*. 2013; 8(3). PMID: [WOS:000317418500043](https://pubmed.ncbi.nlm.nih.gov/WOS:000317418500043/).
18. Schock TB, Stancyk DA, Thibodeaux L, Burnett KG, Burnett LE, Boroujerdi AFB, et al. Metabolomic analysis of Atlantic blue crab, *Callinectes sapidus*, hemolymph following oxidative stress. *Metabolomics*. 2010; 6(2):250–62. PMID: [WOS:000277298700009](https://pubmed.ncbi.nlm.nih.gov/WOS:000277298700009/).
19. Jones OAH, Dondero F, Viarengo A, Griffin JL. Metabolic profiling of *Mytilus galloprovincialis* and its potential applications for pollution assessment. *Marine Ecology Progress Series*. 2008; 369:169–79. doi: [10.3354/meps07654](https://doi.org/10.3354/meps07654)
20. Tuffnail W, Mills G, Cary P, Greenwood R. An environmental 1H NMR metabolomic study of the exposure of the marine mussel *Mytilus edulis* to atrazine, lindane, hypoxia and starvation. *Metabolomics*. 2009; 5:33–43. doi: [10.1007/s11306-008-0143-1](https://doi.org/10.1007/s11306-008-0143-1)
21. Watanabe M, Meyer K, Jackson T, Schock T, Johnson WE, Bearden D. Application of NMR-based metabolomics for environmental assessment in the Great Lakes using zebra mussel (*Dreissena polymorpha*). *Metabolomics*. 2015; 11(5):1302–15. doi: [10.1007/s11306-015-0789-4](https://doi.org/10.1007/s11306-015-0789-4) PMID: [26366138](https://pubmed.ncbi.nlm.nih.gov/26366138/)
22. Dove ADM, Leisen J, Zhou M, Byrne JJ, Lim-Hing K, Webb HD, et al. Biomarkers of Whale Shark Health: A Metabolomic Approach. *PLoS ONE*. 2012; 7(11):e49379. doi: [10.1371/journal.pone.0049379](https://doi.org/10.1371/journal.pone.0049379) PMID: [23166652](https://pubmed.ncbi.nlm.nih.gov/23166652/)
23. Niemuth JN, Stoskopf MK. Hepatic metabolomic investigation of the North American black bear (*Ursus americanus*) using 1H-NMR spectroscopy. *Wildlife Biology in Practice*. 2014; 10(1):14–23. doi: [10.2461/wbp.2014.10.3](https://doi.org/10.2461/wbp.2014.10.3)

24. Gottschalk M, Ivanova G, Collins DM, Eustace A, O'Connor R, Brougham DF. Metabolomic studies of human lung carcinoma cell lines using in vitro (1)H NMR of whole cells and cellular extracts. *NMR in biomedicine*. 2008; 21(8):809–19. doi: [10.1002/nbm.1258](https://doi.org/10.1002/nbm.1258) PMID: [18470962](https://pubmed.ncbi.nlm.nih.gov/18470962/)
25. Bligh EG, Dyer WJ. A rapid method of total lipid extraction and purification. *Canadian journal of biochemistry and physiology*. 1959; 37(8):911–7. PMID: [13671378](https://pubmed.ncbi.nlm.nih.gov/13671378/).
26. Wu H, Southam AD, Hines A, Viant MR. High-throughput tissue extraction protocol for NMR- and MS-based metabolomics. *Analytical biochemistry*. 2008; 372(2):204–12. doi: [10.1016/j.ab.2007.10.002](https://doi.org/10.1016/j.ab.2007.10.002) PMID: [17963684](https://pubmed.ncbi.nlm.nih.gov/17963684/).
27. Benjamini Y, Hochberg Y. Controlling the False Discovery Rate: A Practical and Powerful Approach to Multiple Testing. *Journal of the Royal Statistical Society Series B (Methodological)*. 1995; 57(1):289–300.
28. Wishart DS, Tzur D, Knox C, Eisner R, Guo AC, Young N, et al. HMDB: the Human Metabolome Database. *Nucleic acids research*. 2007; 35(Database issue):D521–6. doi: [10.1093/nar/gkl923](https://doi.org/10.1093/nar/gkl923) PMID: [17202168](https://pubmed.ncbi.nlm.nih.gov/17202168/); PubMed Central PMCID: PMC1899095.
29. Cui Q, Lewis IA, Hegeman AD, Anderson ME, Li J, Schulte CF, et al. Metabolite identification via the Madison Metabolomics Consortium Database. *Nature biotechnology*. 2008; 26(2):162–4. doi: [10.1038/nbt0208-162](https://doi.org/10.1038/nbt0208-162) PMID: [18259166](https://pubmed.ncbi.nlm.nih.gov/18259166/).
30. Ulrich EL, Akutsu H, Doreleijers JF, Harano Y, Ioannidis YE, Lin J, et al. BioMagResBank. *Nucleic acids research*. 2008; 36(Database issue):D402–8. PMID: [17984079](https://pubmed.ncbi.nlm.nih.gov/17984079/).
31. Smith JE, Chavey PS, Miller RE. Iron Metabolism in Captive Black (*Diceros bicornis*) and White (*Ceratotherium simum*) Rhinoceroses. *Journal of Zoo and Wildlife Medicine*. 1995; 26(4):525–31.
32. Yamato M, Muto Y, Yoshida T, Kato M, Moriwaki H. Clearance rate of plasma branched-chain amino acids correlates significantly with blood ammonia level in patients with liver cirrhosis. *International Hepatology Communications*. 1995; 3(2):91–6. [http://dx.doi.org/10.1016/0928-4346\(94\)00159-3](http://dx.doi.org/10.1016/0928-4346(94)00159-3).
33. Kuwahata M, Yoshimura T, Sawai Y, Amano S, Tomoe Y, Segawa H, et al. Localization of polypyrimidine-tract-binding protein is involved in the regulation of albumin synthesis by branched-chain amino acids in HepG2 cells. *The Journal of nutritional biochemistry*. 2008; 19(7):438–47. Epub 2007/08/21. doi: [10.1016/j.jnutbio.2007.05.011](https://doi.org/10.1016/j.jnutbio.2007.05.011) PMID: [17707630](https://pubmed.ncbi.nlm.nih.gov/17707630/).
34. Nishitani S, Ijichi C, Takehana K, Fujitani S, Sonaka I. Pharmacological activities of branched-chain amino acids: specificity of tissue and signal transduction. *Biochem Biophys Res Commun*. 2004; 313(2):387–9. Epub 2003/12/20. PMID: [14684173](https://pubmed.ncbi.nlm.nih.gov/14684173/).
35. She P, Reid TM, Bronson SK, Vary TC, Hajnal A, Lynch CJ, et al. Disruption of BCATm in mice leads to increased energy expenditure associated with the activation of a futile protein turnover cycle. *Cell Metab*. 2007; 6(3):181–94. Epub 2007/09/05. doi: [10.1016/j.cmet.2007.08.003](https://doi.org/10.1016/j.cmet.2007.08.003) PMID: [17767905](https://pubmed.ncbi.nlm.nih.gov/17767905/); PubMed Central PMCID: PMC1893888.
36. Nishitani S, Matsumura T, Fujitani S, Sonaka I, Miura Y, Yagasaki K. Leucine promotes glucose uptake in skeletal muscles of rats. *Biochem Biophys Res Commun*. 2002; 299(5):693–6. Epub 2002/12/10. PMID: [12470633](https://pubmed.ncbi.nlm.nih.gov/12470633/).
37. Muto Y, Sato S, Watanabe A, Moriwaki H, Suzuki K, Kato A, et al. Overweight and obesity increase the risk for liver cancer in patients with liver cirrhosis and long-term oral supplementation with branched-chain amino acid granules inhibits liver carcinogenesis in heavier patients with liver cirrhosis. *Hepatology research: the official journal of the Japan Society of Hepatology*. 2006; 35(3):204–14. Epub 2006/06/02. doi: [10.1016/j.hepres.2006.04.007](https://doi.org/10.1016/j.hepres.2006.04.007) PMID: [16737844](https://pubmed.ncbi.nlm.nih.gov/16737844/).
38. Korenaga M, Nishina S, Korenaga K, Tomiyama Y, Yoshioka N, Hara Y, et al. Branched-chain amino acids reduce hepatic iron accumulation and oxidative stress in hepatitis C virus polyprotein-expressing mice. *Liver international: official journal of the International Association for the Study of the Liver*. 2015; 35(4):1303–14. Epub 2014/08/27. doi: [10.1111/liv.12675](https://doi.org/10.1111/liv.12675) PMID: [25156780](https://pubmed.ncbi.nlm.nih.gov/25156780/); PubMed Central PMCID: PMC1893888.
39. James JH, Ziparo V, Jeppsson B, Fischer JE. Hyperammonaemia, plasma aminoacid imbalance, and blood-brain aminoacid transport: a unified theory of portal-systemic encephalopathy. *Lancet (London, England)*. 1979; 2(8146):772–5. Epub 1979/10/13. PMID: [90864](https://pubmed.ncbi.nlm.nih.gov/90864/).
40. Dejong CH, van de Poll MC, Soeters PB, Jalan R, Olde Damink SW. Aromatic amino acid metabolism during liver failure. *The Journal of nutrition*. 2007; 137(6 Suppl 1):1579S–85S; discussion 97S-98S. Epub 2007/05/22. PMID: [17513430](https://pubmed.ncbi.nlm.nih.gov/17513430/).
41. Fischer JE, Yoshimura N, Aguirre A, James JH, Cummings MG, Abel RM, et al. Plasma amino acids in patients with hepatic encephalopathy. Effects of amino acid infusions. *Am J Surg*. 1974; 127(1):40–7. Epub 1974/01/01. PMID: [4808685](https://pubmed.ncbi.nlm.nih.gov/4808685/).
42. Soeters PB, Fischer JE. Insulin, glucagon, aminoacid imbalance, and hepatic encephalopathy. *Lancet (London, England)*. 1976; 2(7991):880–2. Epub 1976/10/23. PMID: [62115](https://pubmed.ncbi.nlm.nih.gov/62115/).

43. Tajiri K, Shimizu Y. Branched-chain amino acids in liver diseases. *World Journal of Gastroenterology: WJG*. 2013; 19(43):7620–9. doi: [10.3748/wjg.v19.i43.7620](https://doi.org/10.3748/wjg.v19.i43.7620) PMID: [PMC3837260](https://pubmed.ncbi.nlm.nih.gov/23837260/).
44. Beben T, Rifkin DE. GFR Estimating Equations and Liver Disease. *Advances in chronic kidney disease*. 2015; 22(5):337–42. Epub 2015/08/28. doi: [10.1053/j.ackd.2015.05.003](https://doi.org/10.1053/j.ackd.2015.05.003) PMID: [26311594](https://pubmed.ncbi.nlm.nih.gov/26311594/); PubMed Central PMCID: [PMCPmc4552961](https://pubmed.ncbi.nlm.nih.gov/PMC4552961/).
45. Caregaro L, Menon F, Angeli P, Amodio P, Merkel C, Bortoluzzi A, et al. Limitations of serum creatinine level and creatinine clearance as filtration markers in cirrhosis. *Archives of internal medicine*. 1994; 154(2):201–5. Epub 1994/01/24. PMID: [8285815](https://pubmed.ncbi.nlm.nih.gov/8285815/).
46. MacAulay J, Thompson K, Kiberd BA, Barnes DC, Peltekian KM. Serum creatinine in patients with advanced liver disease is of limited value for identification of moderate renal dysfunction: Are the equations for estimating renal function better? *Canadian Journal of Gastroenterology*. 2006; 20(8):521–6. PMID: [PMC2659934](https://pubmed.ncbi.nlm.nih.gov/PMC2659934/).
47. Serra MA, Puchades MJ, Rodriguez F, Escudero A, del Olmo JA, Wassel AH, et al. Clinical value of increased serum creatinine concentration as predictor of short-term outcome in decompensated cirrhosis. *Scandinavian journal of gastroenterology*. 2004; 39(11):1149–53. Epub 2004/11/17. doi: [10.1080/00365520410008024](https://doi.org/10.1080/00365520410008024) PMID: [15545175](https://pubmed.ncbi.nlm.nih.gov/15545175/).
48. Parsons HM, Ekman DR, Collette TW, Viant MR. Spectral relative standard deviation: a practical benchmark in metabolomics. *The Analyst*. 2009; 134:478–85. doi: [10.1039/b808986h](https://doi.org/10.1039/b808986h) Epub 2008 Dec 2. PMID: [19238283](https://pubmed.ncbi.nlm.nih.gov/19238283/).